Published in final edited form as:
J Comp Neurol. 2014 March ; 522(4): 844–860. doi:10.1002/cne.23448.

Variable temporo-insular cortex neuroanatomy in primates suggests a bottleneck effect in eastern gorillas

Sarah K. Barks[1], **Amy L. Bauernfeind**[1], **Christopher J. Bonar**[2], **Michael R. Cranfield**[3], **Alexandra A. de Sousa**[4], **Joseph M. Erwin**[1], **William D. Hopkins**[5,6], **Albert H. Lewandowski**[7], **Antoine Mudakikwa**[8], **Kimberley A. Phillips**[9], **Mary Ann Raghanti**[10], **Cheryl D. Stimpson**[1], **Patrick R. Hof**[11,12], **Karl Zilles**[13,14,15], and **Chet C. Sherwood**[1]

[1]Center for the Advanced Study of Hominid Paleobiology and Department of Anthropology, The George Washington University, Washington DC 20052 [2]Dallas Zoo, Dallas, TX 75203 [3]Mountain Gorilla Veterinary Project, School of Veterinary Medicine, University of California Davis, Davis, CA 95616 [4]Department of Life Sciences, University of Coimbra, 3001-056 Coimbra, Portugal [5]Neuroscience Institute, Georgia State University, Atlanta, GA 30303 [6]Division of Developmental and Cognitive Neuroscience, Yerkes National Primate Research Center, Atlanta, GA 30329 [7]Cleveland Metroparks Zoo, Cleveland, OH 44109 [8]Rwanda Development Board, Department of Tourism and Conservation, Kigale, Rwanda [9]Department of Psychology, Trinity University, San Antonio, TX 78212 [10]Department of Anthropology and School of Biomedical Sciences, Kent State University, Kent, OH 44240 [11]Fishberg Department of Neuroscience and Friedman Brain Institute, Icahn School of Medicine at Mount Sinai, New York, NY 10029 [12]New York Consortium in Evolutionary Primatology, New York, NY 10024 [13]Institute of Neuroscience and Medicine, Research Center Jülich, 52425 Jülich, Germany [14]C. & O. Vogt Institute of Brain Research, Heinrich-Heine University Düsseldorf, 40225 Düsseldorf, Germany [15]Department of Psychiatry, Psychotherapy, and Psychosomatics, RWTH Aachen University, 52074 Aachen, Germany

Abstract

In this study, we describe an atypical neuroanatomical feature present in several primate species that involves a fusion between the temporal lobe (often including Heschl's gyrus in great apes) and the posterior dorsal insula, such that a portion of insular cortex forms an isolated pocket medial to the Sylvian fissure. We assessed the frequency of this fusion in 56 primate species (including apes, Old World monkeys, New World monkeys, and strepsirrhines) using either magnetic resonance images or histological sections. A fusion between temporal cortex and

Corresponding Author: Sarah K. Barks, Department of Anthropology, The George Washington University, 2110 G St. NW, Washington, DC, Telephone: 202.994.5923, Fax: 202.994.6097, skbarks@gwu.edu.

Conflicts of interest

The authors declare that they have no conflict of interest.

Contributions of authors to the study

All authors had full access to the data in the study and take responsibility for the integrity of the data and the accuracy of the data analysis. Study concept and design: S.K.B., A.L.B., C.J.B., M.R.C., A.A.d.S., J.M.E., P.R.H., W.D.H., A.H.L., A.M., K.A.P., M.A.R., C.C.S., C.D.S., K.Z. Acquisition of data: C.J.B., M.R.C., J.M.E., A.A.d.S., P.R.H., W.D.H., A.H.L., A.M., K.A.P., M.A.R., C.C.S., C.D.S., K.Z. Analysis and interpretation of data: S.K.B., A.L.B., K.A.P., M.A.R., C.C.S. Drafting of the manuscript: S.K.B., A.L.B. Critical revision of the manuscript for important intellectual content: P.R.H., M.A.R., C.C.S., K.Z. Obtained funding: A.A.d.S., J.M.E., P.R.H., W.D.H., K.A.P., M.A.R., C.C.S. Administrative, technical, and material support: J.M.E., A.M. Study supervision: C.C.S.

posterior insula was present in 22 species (7 apes, 2 Old World monkeys, 4 New World monkeys, and 9 strepsirrhines). The temporo-insular fusion was observed in most eastern gorilla (*Gorilla beringei beringei* and *G. b. graueri*) specimens (62% and 100% of cases, respectively) but less frequently in other great apes and was never found in humans. We further explored the histology of this fusion in eastern gorillas by examining the cyto- and myeloarchitecture within this region, and observed that the degree to which deep cortical layers and white matter are incorporated into the fusion varies among individuals within a species. We suggest that fusion between temporal and insular cortex is an example of a relatively rare neuroanatomical feature that has become more common in eastern gorillas, possibly as the result of a population bottleneck effect. Characterizing the phylogenetic distribution of this morphology highlights a derived feature of these great apes.

Keywords

cerebral cortex; cortical fusion; auditory cortex; ape

Introduction

In primates, the expansion of the frontoparietal and temporal opercula creates the Sylvian fissure, a sulcus located on the lateral surface of the cerebral hemispheres. The insular cortex is located within the Sylvian fissure, bound by the superior and inferior limiting sulci (Cunningham, 1897; Mesulam and Mufson, 1982; Naidich et al., 2004). In this study, we describe an atypical feature of the neuroanatomy of this region that occurs in some primates involving a fusion of cortex that bridges the posterior temporal lobe (often including Heschl's gyrus in great apes) and the posterior dorsal insula. Characterizing the phylogenetic distribution of this rare morphologic feature can highlight instances in primates where genetic drift and population bottleneck effects—i.e., a significant decrease in population numbers resulting in a reduction of genetic diversity—may have led to its fixation within a relatively small and isolated species.

Despite the close spatial proximity of the superior temporal cortex and posterior insula, it is unusual to observe the anatomical fusion of these functionally distinct cortical regions. The posterior insular cortex is the target of dense thalamocortical inputs (Craig, 2003) and displays activation in response to a variety sensory inputs, including hunger, thirst, touch, and pain (Ostrowsky et al., 2002; Craig, 2003, 2010). In primates, the posterior extent of the superior temporal gyrus (STG) comprises the primary auditory cortex and auditory association cortices (Galaburda and Sanides, 1980; Hackett et al., 2001; Smiley et al., 2007).

While the primate insular cortex as a whole is divided into several subregions based on variation in cytoarchitecture (Rose, 1928; Mesulam and Mufson, 1982; Carmichael and Price, 1994; Gallay et al., 2011; Morel et al., 2013), the posterior insular cortex is granular in composition, containing small, densely packed neurons in layer IV (Mesulam and Mufson, 1982; Preuss and Goldman-Rakic, 1991; Carmichael and Price, 1994; Kurth et al., 2010; Bauernfeind et al., 2013). In macaque monkeys (i.e., *Macaca mulatta*, *M. fascicularis*) and humans, myelin staining reveals dense radial fibers within the deep cortical layers (layers IV–VI) (Mesulam and Mufson, 1982; Gallay et al., 2011; Morel et al., 2013). The

primary auditory cortex, like the posterior insular cortex, is characterized by dense packing of neurons in layer IV (Galaburda and Sanides, 1980; Hackett et al., 2001; Morosan et al., 2001) with a heavy degree of myelination (Wallace et al., 1991; Smiley et al., 2007). The primary auditory cortex lies both medial and lateral to a belt of association cortical areas (Kaas and Hackett, 2000; Hackett et al., 2001), where decreased staining for myelin is observed relative to the primary auditory core, particularly in cortical layer IV (Hackett et al., 2001). As a primary sensory cortical area, the auditory cortex mainly receives thalamocortical input from the medial geniculate complex (Kaas and Hackett, 2000; Smiley et al., 2007); medial association areas, in contrast, receive corticocortical inputs from somatosensory cortex in addition to thalamocortical auditory input (Kaas and Hackett, 2000; Schroeder et al., 2001; Smiley et al., 2007).

Here we report the distribution of an uncommon temporo-insular fusion in several primate species using both structural neuroimaging and histology.

Materials and Methods

Sample

We examined a total of 56 primate species representing apes (11 species), Old World monkeys (15 species), New World monkeys (17 species), and strepsirrhines (13 species), including 403 individuals in total, using both magnetic resonance imaging (MRI) and histological samples of Nissl-stained sections. Sample sizes within species vary from n = 1 to n = 103 (see Table 1 for details). Specimens were obtained from the following sources: multiple zoos in the United States; primate research facilities including the Yerkes National Primate Research Center, the National Primate Research Center at the University of Washington, the Southwest National Primate Research Center, and the University of Texas M.D. Anderson Cancer Center; the Mountain Gorilla Veterinary Project (Davis, CA) and the Gorilla Foundation (Woodside, CA); the Great Ape Aging Project and the Zilles and Stephan comparative neuroanatomy collections at the C. & O. Vogt Institute of Brain Research in Düsseldorf, Germany; online resources including the University of Wisconsin and Michigan State Comparative Mammalian Brain Collections (http://brainmuseum.org), the UCLA Laboratory of Neuro Imaging (http://www.loni.ucla.edu/Atlases/index.jsp), BrainMaps.org (Mikula et al., 2008), and the Open Access Series of Imaging Studies (Marcus et al., 2007); and primate brain atlases (Gergen and MacLean, 1962; Bons et al., 1998; Paxinos et al., 2009; Hardman and Ashwell, 2012; Paxinos et al., 2012). Captive animals from which we obtained brains for this study were housed according to the ethical guidelines of their respective institutions, following approval by the relevant Institutional Animal Care and Use Committee (IACUC) protocols. All animals in this study died of non-neurological causes unrelated to our research.

A large subsample of these specimens was from a wild population of mountain gorillas (n = 21) in the Volcanoes National Park in Rwanda, monitored daily by the Rwanda Development Board, the Dian Fossey Gorilla Fund International's Karisoke Research Center, and the Mountain Gorilla Veterinary Project. When deceased mountain gorilla remains were encountered during such daily monitoring (typically within 24 hours of death),

a postmortem necropsy examination was performed, which included collection of brain tissue when preservation conditions permitted it.

Structural neuroimaging

The MRIs used in this study were acquired over several years at multiple institutions, using a wide range of scanners (ranging from 1.5 to 9.4 T) and imaging parameters, and included both postmortem and *in vivo* specimens (see e.g. Hopkins et al., 2007; Hopkins et al., 2009; Phillips and Thompson, 2013). Presence or absence of a fusion between the superior temporal cortex and insular cortex was assessed in each individual MR image in the coronal plane, where it is most easily identified (Galaburda and Sanides, 1980). Additional orientation planes were consulted when observation of fusion morphology presented difficulty in the coronal plane. In order to make a positive identification of a fusion in a specimen, a connection between the superior temporal cortex and the posterior insular cortex must create a visible open space inferior to the point of fusion as viewed coronally. When poor imaging resolution prevented the determination of whether a fusion occurred and a histological sample was not available, the specimen was excluded from the study. Five raters assessed presence or absence of a fusion in each hemisphere of a subset of 16 great ape MR images, yielding 93.75% overall agreement and a free-marginal Kappa statistic of 0.917.

Histology

Nissl-stained coronal sections were examined under brightfield illumination on a Zeiss Axioplan 2 microscope and assessed for presence of a temporo-insular fusion. Two criteria were used to identify the presence of a fusion. First, tissue of the superior temporal cortex and posterior insular cortex fusion must include cortical layers deeper than layer I, such that the fusion extends into the layers of the cortex. Second, an “island” of insular cortex must be isolated below the point of fusion, leaving a central space. Many strepsirrhines lack a fully developed superior limiting sulcus, but instead have a homologous dimple in their cortical surface (Bauernfeind et al., 2013). In these species, the homologous dimple was used to determine the dorsal extent of insular cortex. In 14 species, only one hemisphere was available for study and therefore laterality could not be fully assessed. When both MRI and histological data were available for a specimen, that specimen was categorized based on histology due to its higher anatomical resolution. We were able to determine with confidence that MRIs and histological results produced comparable results regarding identification of the presence or absence of this insular fusion by direct comparison of examples of each data type within individuals for which the intact brain had been imaged prior to sectioning and staining.

We further explored the cytoarchitecture of the site of fusion in a subset of mountain gorillas (n = 6, including two specimens with connections containing white matter), a Grauer’s gorilla, and a pigtail macaque by staining for myelin, which is abundantly present in layers IV through VI within both posterior insular and primary auditory cortices. Tissue blocks were cryoprotected by immersion in buffered sucrose solutions up to 30%, embedded in Tissue-Tek medium, frozen in a slur of dry ice and isopentane, and sectioned at 40 μm with a sliding microtome, then stained using the Gallyas method (1971).

When both hemispheres were available, the occurrence of a fusion was documented in each hemisphere and the frequency of laterality was calculated as a percentage of total sample size. Specimens for which only one hemisphere was available were not included in this assessment.

Photomicography

We used StereoInvestigator 10.2 (MBF Bioscience, Williston, VT) to obtain photomicrographs of histology using an Optronics MicroFire digital camera mounted on a Zeiss Axioplan 2 microscope. Brightness and contrast of images were adjusted with Adobe Photoshop Elements 4.0 software (San Jose, CA). Adobe Illustrator 8.0 and Microsoft PowerPoint 14 were used to assemble and label figures.

Phylogenetic reconstruction

The phylogenetic distribution of the temporo-insular fusion was documented within great apes. Small sample size prevented phylogenetic analyses including other taxa. A phylogenetic tree of the primates included in this study was obtained from the 10kTrees project (Arnold et al., 2010, version 3). The evolution of this trait was optimized to the tree using maximum parsimony analysis with character state transformations unordered, using Mesquite software version 2.75 (Maddison and Maddison, 2011). The temporo-insular fusion trait was characterized as common (present in 60% or more specimens within the species), intermediate (present in 30–59% of specimens), or rare or absent (present in 0–29% of specimens).

Results

Frequency and distribution

Of the 56 primate species in this study, 22 (7 apes, 2 Old World monkeys, 4 New World monkeys, and 9 strepsirrhines) displayed the presence of a fusion between temporal and insular cortices creating a pocket of isolated cortex in one or both hemispheres in at least one specimen (Table 1). Fusions were equally likely to occur bilaterally or unilaterally without directional bias (Fig. 1). While this fusion appears to be rare in monkeys, it occurred fairly frequently in our sample of strepsirrhines and was present in at least one specimen of all great ape species except humans. Great apes represented the largest sample size in this study, and the frequency of the temporo-insular fusion was highly variable among these species: it was most prevalent in the two eastern gorilla species (62% and 100% of cases in mountain gorillas and Grauer’s gorillas, respectively) and occured with intermediate frequency in western lowland gorillas (*Gorilla gorilla gorilla*), bonobos (*Pan paniscus*), and orangutans (*Pongo pygmaeus*) (53%, 50%, and 25% of cases, respectively). The temporo-insular fusion was absent in humans (*Homo sapiens*) and was extremely rare in chimpanzees (*Pan troglodytes*), occurring in only 6 out of 102 subjects (6% of cases). Phylogenetic analysis (Fig. 2) suggested that the temporo-insular fusion was rare in the last common ancestor of hominoids and has remained so in chimpanzees, humans, and orangutans, but has become more common in gorillas (particularly eastern gorillas). Its intermediate frequency in bonobos may represent parallel evolution with gorillas.

Anatomy and histology

Examples of fused temporo-insular anatomy as seen in MRI are presented in Figure 3, depicting a Grauer's gorilla in coronal sections, with corresponding tissue stained for myelin, and Figure 4, depicting a series of parasagittal MRI sections from a mountain gorilla. Examples of typical unfused anatomy are presented in Figure 5, showing a chimpanzee in coronal sections, and Figure 6, illustrating a human in parasagittal sections. Further examples of fused and unfused temporo-insular anatomy in many great apes are shown in Figures 7–10. When the temporo-insular fusion was present, a distinctive projection of Heschl's gyrus was visible in the parasagittal plane as seen in Figures 4, 7A, 7B, 8A, 8B, and 9A. When an isolated pocket of cortex appeared, it did not typically re-open; that is, the inferior limiting sulcus of the insula closed at the posterior extent of the pocket as the posterior temporal cortex met the parietal operculum. While we only counted a fusion as occurring if layer II or deeper was involved, there was significant variation in the extent of cortical depth (i.e., number of cortical layers included) of the temporo-insular fusion across subjects and species (Figs. 11 and 12). The degree to which deeper cortical layers were involved in the temporal-insular fusion typically increased in more posterior coronal sections, and sometimes included subcortical white matter. The site of fusion within the posterior insula also varied across subjects and species (Figs. 11 and 12), but typically occurred in the dorsal posterior insular cortex.

We further explored the cytoarchitecture of the temporo-insular fusion in a subset of mountain gorillas and one Grauer's gorilla. An example of a typical gray matter fusion in a mountain gorilla stained for both cytoarchitecture and myelin is shown in Figure 13A and B (Nissl substance) and 13C (myelin). A fusion in a second mountain gorilla which includes white matter is shown in Figure 13D and E (Nissl substance) and 13F (myelin); this same fusion stained for Nissl substance is shown at higher magnification in Figure 14. Finally, a cortical fusion (without white matter) in a pigtail macaque is shown in Figure 13G–I. When the fusion included layer IV or deeper cortical layers, the dense radial fibers in myelin staining and granularity of cortical layer IV seen in both core primary auditory and posterior insular cortices extended into the tissue forming the bridge between these two areas (Fig. 14). The isolated pocket or "island" of cortex inferior to this bridge is characterized by a densely stained but relatively narrow granular layer IV, as is typical of the posterior granular insula. Myelin staining in this area was more diffuse than in the bridge of tissue and denser in the lateral side of the island, corresponding to the medial surface of Heschl's gyrus in great apes, inferior to the core of primary auditory cortex.

Discussion

This study evaluated the prevalence of a rare variant of the temporo-insular neuroanatomy across a broad sample of primates. We observed a fusion between auditory and posterior insular cortices that was more frequent in eastern gorillas than in the other great apes we studied, and varied in the extent to which deep cortical layers and white matter fibers were included within the fusion. This fusion is particularly unusual as it involves a direct connection between a primary sensory cortex and a distinctly different higher-order

association cortex from a different sensory modality, which has not previously been observed.

The MRI data used in this study vary considerably in spatial resolution, and we acknowledge some potential sources of error in interpreting MR results. It is possible that due to low MR resolution or partial volume effects (which occur when a given voxel in an MR image straddles the boundary between tissue types—e.g. white and gray matter—resulting in an intermediate intensity value) we have in some cases identified a cortical fusion where one does not in fact exist. However, in all cases for which we have both histological and MR data, a temporo-insular cortical fusion identified in the MR image was also observed in the corresponding histological section. As such, we believe that our results reflect a real biological phenomenon in these data. MR images with spatial resolution too poor to definitively characterize the presence or absence of a fusion were not included in this study.

One factor that might contribute to the appearance of this relatively uncommon fusion is cortical gyrification. Gyrification — the degree to which the cortex is folded — increases in anthropoids with larger neocortical volume (Zilles et al., 1989; 2013). Among primates, the gyrification index (the ratio of total cortical area, including that which is buried in sulci, to surface cortical area (Zilles et al., 1988) is highest in the great apes. Humans show the highest levels of gyrification in the parietal association cortex and the superior surface of the posterior temporal lobe (i.e., auditory cortex including Wernicke's area) (Zilles et al., 1988). The tension-based theory of morphological development proposes that gyrification of the neocortex occurs due to tension in white matter tracts that draws interconnected regions of cortex closer (Dehay et al., 1996; Van Essen, 1997; Dehay and Kennedy, 2007; Zilles et al., 2013). A fusion between the auditory and posterior insular cortices, often containing a white matter tract, suggests that these two regions may be functionally connected. Indeed, the posterior insular cortex of macaques is known to be interconnected with the superior temporal cortex and auditory areas based on horseradish peroxide injections (Mesulam and Mufson, 1985), a finding that may pertain to the role of the insular cortex as a mediator of auditory information (Bamiou et al., 2003).

Fusions between adjacent gyri have been observed in the human inferior frontal cortex (Amunts et al. 1999), and Galaburda and Sanides (1980) described in three human subjects variable extensions of the superior temporal cortex into the parietal cortex that created isolated cortical pockets, including a fusion between the planum temporale and superior insular cortex in one subject that is similar to the fusion we have described in this study; they attributed this connection to the high degree of folding in that region. It is evident, therefore, that this temporo-insular fusion might be present in a small minority of humans. However, our exploration of a very large human sample indicated that its presence is quite rare in this species. Much like humans, other great apes have the highest levels of gyrification in the posterior temporal lobe and parietal lobe (Zilles et al., 1988, 1989). While increased gyrification might contribute to the formation of temporo-insular cortex fusion in great apes, the more common appearance of this trait in strepsirrhines compared to Old World monkeys or humans suggests that other factors are likely to play a role as well. Developmental cortical folding processes are thought to be controlled by only a few genes

(Pilz et al., 1998; Kato and Dobyns, 2003), one or more of which could vary in its expression across primate phylogeny.

Fusion between the posterior superior temporal and the insular cortices appears to be rare or absent in most haplorrhine primates, but fairly common in eastern gorillas. The distribution of this fusion may have been the result of a recent bottleneck in the population, which led to substantially reduced numbers of gorillas. With population bottlenecks, the prevalence of a rare variant of a trait can increase rapidly in a small gene pool by genetic drift. This phenomenon has been observed in a number of species; for instance, spread of atypical asymmetry in cranial features followed an apparent population bottleneck in northern elephant seals (Hoelzel, 1999), while two bottlenecks (one in the late Pleistocene, one likely in the 19th century) in cheetahs putatively caused the extremely low genetic diversity present in that species today (O'Brien et al., 1987). Each of the two eastern gorilla species has a very small population size, totaling approximately 880 mountain gorillas based on the most recent census data from the Bwindi Impenetrable Forest in Uganda and the Virunga volcanoes in Rwanda (Robbins et al., 2011) and approximately 5,000 Grauer's gorillas in the Democratic Republic of the Congo (DRC) (Berggorilla und Regenwald Direkthilfe, 2012), although accurate census data are particularly difficult to obtain in DRC due to ongoing conflicts in the area. Genetic studies suggest that both eastern gorilla populations have undergone reduction in the recent past (Jensen-Seaman and Kidd, 2001) and each has less genetic diversity than the larger, more widespread western lowland gorilla population (Jensen-Seaman et al., 2003; Bergl et al., 2008).

While the fusion of temporal and insular cortices was commonly observed in eastern gorillas in this study and somewhat frequently in other ape species, it was rarely seen in monkeys. Intriguingly, however, it did appear in most strepsirrhine species studied here. A more in-depth exploration of the cytoarchitecture and connectivity of this fused region and adjacent cortex in strepsirrhines would be valuable in order to elucidate its relationship with the same feature in great apes. Given their phylogenetic distance, it is most likely that the temporo-insular fusion evolved independently in the ape and strepsirrhine lineages. Additionally, while this study examines a wide range of primate species, it is limited in sample size beyond the great apes. Future investigation of larger sample sizes in monkey and strepsirrhine species would help to further characterize the phylogenetic distribution of this morphology.

Acknowledgments

Grant sponsor: National Science Foundation; Grant numbers: BCS-0515484, BCS-0549117, BCS-0824531, BCS-0921079, and DGE-0801634; Grant sponsor: National Institutes of Health; Grant numbers: AG14308, R15NS070717-01, RR00166, and RR013986; Grant sponsor: the James S. McDonnell Foundation; Grant numbers: 22002078 and 220020293; Grant sponsor: the Portuguese Science and Technology Federation (FCT); Grant number: SFRH/BPD/43518/2008.

The Mammalian Brain Collection is supported by the National Science Foundation and the National Institutes of Health. We thank Dr. John Allman for assistance with the histological preparation of one *Gorilla beringei graueri* brain, Dr. Aida Gómez-Robles for assistance with figures, and two anonymous reviewers for helpful comments on a previous draft.

Literature cited

Amunts K, Schleicher A, Bürgel U, Mohlberg H, Uylings HBM, Zilles K. Broca's region revisited: cytoarchitecture and intersubject variability. J Comp Neurol. 1999; 412:319–341. [PubMed: 10441759]

Arnold C, Matthews LJ, Nunn CL. The 10ktrees website: a new online resource for primate phylogeny. Evol Anthropol. 2010; 19:114–118.

Bamiou D-E, Musiek FE, Luxon LM. The insula (island of Reil) and its role in auditory processing. Brain Res Rev. 2003; 42:143–154. [PubMed: 12738055]

Bauernfeind AL, de Sousa AA, Avasthi T, Dobson SD, Raghanti MA, Lewandowski AH, Zilles K, Semendeferi K, Allman JM, Craig AD, Hof PR, Sherwood CC. A volumetric comparison of the insular cortex and its subregions in primates. J Hum Evol. 2013; 64:263–279. [PubMed: 23466178]

Bergl RA, Bradley BJ, Nsubuga A, Vigilant L. Effects of habitat fragmentation, population size and demographic history on genetic diversity: the Cross River gorilla in a comparative context. Am J Primatol. 2008; 70:848–859. [PubMed: 18521886]

[Accessed February 19, 2012] Berggorilla und Regenwald Direkthilfe. http://berggorilla.de/index.php?id=824&L=1

Bons, N.; Silhol, S.; Barbié, V.; Mestre-Francés, N.; Albe-Fessard, D. A stereotaxic atlas of the grey lesser mouse lemur brain (Microcebus murinus). New York: Elsevier; 1998.

Carmichael ST, Price JL. Architectonic subdivision of the orbital and medial prefrontal cortex in the macaque monkey. J Comp Neurol. 1994; 346:366–402. [PubMed: 7527805]

Craig AD. Interoception: the sense of the physiological condition of the body. Curr Opin Neurobiol. 2003; 13:500–505. [PubMed: 12965300]

Craig AD. The sentient self. Brain Struct Funct. 2010; 214:563–577. [PubMed: 20512381]

Cunningham FRS. The insular district of the cerebral cortex in man and in the man-like apes. J Anat Physiol. 1897; 32:11–22.

Dehay C, Giroud P, Berland M, Killackey H, Kennedy H. Contribution of thalamic input to the specification of the cytoarchitectonic cortical fields in the primate: effects of bilateral enucleation in the fetal monkey on the boundaries, dimensions, and gyrification of striate and extrastriate cortex. J Comp Neurol. 1996; 367:70–89. [PubMed: 8867284]

Dehay C, Kennedy H. Cell-cycle control and cortical development. Nat Rev Neurosci. 2007; 8:438–450. [PubMed: 17514197]

Galaburda A, Sanides F. Cytoarchitectonic organization of the human auditory cortex. J Comp Neurol. 1980; 190:597–610. [PubMed: 6771305]

Gallay DS, Gallay MN, Jeanmonod D, Rouiller EM, Morel A. The insula of Reil revisited: multiarchitectonic organization in macaque monkeys. Cereb Cortex. 2011; 22:175–190. [PubMed: 21613468]

Gallyas F. A principle for silver staining of tissue elements by physical development. Acta Morphol Acad Sci Hung. 1971; 19:57–71. [PubMed: 4107509]

Gergen, JA.; MacLean, PD. A stereotaxic atlas of the squirrel monkey's brain (Saimiri sciureus). Bethesda, MD: U.S. Department of Health, Education, and Welfare; 1962.

Hackett TA, Preuss TM, Kaas JH. Architectonic identification of the core region in auditory cortex of macaques, chimpanzees, and humans. J Comp Neurol. 2001; 441:197–222. [PubMed: 11745645]

Hardman, CD.; Ashwell, KWS. Stereotaxic and chemoarchitectural atlas of the brain of the common marmoset (Callithrix jacchus). New York: CRC Press; 2012.

Hoelzel AR. Impact of population bottlenecks on genetic variation and the importance of life-history: a case study of the northern elephant seal. Biol J Linn Soc. 1999; 68:23–39.

Hopkins WD, Cantalupo C, Taglialatela J. Handedness is associated with asymmetries in gyrification of the cerebral cortex of chimpanzees. Cereb Cortex. 2007; 17:1750–1756. [PubMed: 17012377]

Hopkins WD, Lyn H, Cantalupo C. Volumetric and lateralized differences in selected brain regions of chimpanzees (*Pan troglodytes*) and bonobos (*Pan paniscus*). Am J Primatol. 2009; 71:988–997. [PubMed: 19760676]

Jensen-Seaman, MI.; Deinard, AS.; Kidd, KK. Mitochondrial and nuclear DNA estimates of divergence between western and eastern gorillas. In: Taylor, A.; Goldsmith, M., editors. Gorilla biology: a multidisciplinary perspective. Cambridge: Cambridge University Press; 2003. p. 247-268.

Jensen-Seaman MI, Kidd KK. Mitochondrial DNA variation and biogeography of eastern gorillas. Mol Ecol. 2001; 10:2241–2247. [PubMed: 11555266]

Kaas JH, Hackett TA. Subdivisions of auditory cortex and processing streams in primates. Proc Natl Acad Sci USA. 2000; 97:11793–11799. [PubMed: 11050211]

Kato M, Dobyns WB. Lissencephaly and the molecular basis of neuronal migration. Hum Mol Genet. 2003; 12:R89–R96. [PubMed: 12668601]

Kurth F, Eickhoff SB, Schleicher A, Hoemke L, Zilles K, Amunts K. Cytoarchitecture and probabilistic maps of the human posterior insular cortex. Cereb Cortex. 2010; 20:1448–1461. [PubMed: 19822572]

Maddison, WP.; Maddison, DR. Mesquite: A modular system for evolutionary analysis. 2011. Version 2.75. http://mesquiteproject.org

Marcus DS, Wang TH, Parker J, Csernansky JG, Morris JC, Buckner RL. Open access series of imaging studies (OASIS): cross-sectional MRI data in young, middle aged, nondemented, and demented older adults. J Cogn Neurosci. 2007; 19:1498–1507. [PubMed: 17714011]

Mesulam MM, Mufson EJ. Insula of the old world monkey. I: architectonics in the insulo-orbito-temporal component of the paralimbic brain. J Comp Neurol. 1982; 212:1–22. [PubMed: 7174905]

Mesulam, MM.; Mufson, EJ. The insula of Reil in man and monkey: architectonics, connectivity and function. In: Jones, EG.; Peters, A., editors. Cerebral Cortex. Vol. 4. New York: Plenum Press; 1985. p. 179-226.

Mikula S, Stone JM, Jones EG. BrainMaps.org—interactive high-resolution digital brain atlases and virtual microscopy. Brains Minds Media. 2008; 3:bmm1426. [PubMed: 19129928]

Morel A, Gallay MN, Baechler A, Wyss M, Gallay DS. The human insula: architectonic organization and postmortem MRI registration. Neuroscience. 2013; 236:117–135. [PubMed: 23340245]

Morosan P, Rademacher J, Schleicher A, Amunts K, Schormann T, Zilles K. Human primary auditory cortex: cytoarchitectonic subdivisions and mapping into a spatial reference system. NeuroImage. 2001; 13:684–701. [PubMed: 11305897]

Naidich TP, Kang E, Fatterpekar GM, Delman BN, Gultekin SH, Wolfe D, Ortiz O, Yousry I, Weismann M, Yousry TA. The insula: anatomic study and MR imaging display at 1.5 T. Am J Neuroradiol. 2004; 25:222–232. [PubMed: 14970021]

O'Brien SJ, Wildt DT, Bush M, Caro TM, FitzGibbon C, Aggundey I, Leakey RE. East African cheetahs: evidence for two population bottlenecks? Proc Natl Acad Sci USA. 1987; 84:508–511. [PubMed: 3467370]

Ostrowsky K, Magnin M, Ryvlin P, Isnard J, Guenot M, Mauguière F. Representation of pain and somatic sensation in the human insula: a study of responses to direct electrical cortical stimulation. Cereb Cortex. 2002; 12:376–385. [PubMed: 11884353]

Paxinos, G.; Huang, X.; Petrides, M.; Toga, AW. The rhesus monkey brain in stereotaxic coordinates. 2. New York: Academic Press; 2009.

Paxinos, G.; Watson, C.; Petrides, M.; Rosa, M.; Tokuno, H. The marmoset brain in stereotaxic coordinates. New York: Elsevier; 2012.

Pilz DT, Matsumoto N, Minnerath S, Mills P, Gleeson JG, Allen KM, Walsh CA, Barkovich AJ, Dobyns WB, Ledbetter DH, Ross ME. *LIS1* and *XLIS* (*DCX*) mutations cause most classical lissencephaly, but different patterns of malformation. Hum Mol Genet. 1998; 7:2029–2037. [PubMed: 9817918]

Phillips KA, Thompson CR. Hand preference for tool-use in capuchin monkeys (*Cebus apella*) is associated with asymmetry of the primary motor cortex. Am J Primatol. 2013; 75:435–440. [PubMed: 22987442]

Preuss TM, Goldman-Rakic PS. Myelo- and cytoarchitecture of the granular frontal cortex and surrounding regions in the strepsirhine primate *Galago* and the anthropoid primate *Macaca*. J Comp Neurol. 1991; 310:429–474. [PubMed: 1939732]

Robbins, MM.; Roy, J.; Write, E.; Kato, R.; Kabano, P.; Basabose, A.; Tibenda, E.; Vigilant, L.; Gray, G. Bwindi mountain gorilla census 2011 — Summary of results. Uganda Wildlife Authority; 2011.

Rose M. Die Inselrinde des Menschen und der Tiere. J Psychol Neurol. 1928; 37:467–624.

Schroeder CE, Lindsley RW, Specht C, Marcovici A, Smiley JF, Javitt DC. Somatosensory input to auditory association cortex in the macaque monkey. J Neurophysiol. 2001; 85:1322–1327. [PubMed: 11248001]

Smiley JF, Hackett TA, Ulbert I, Karmas G, Lakatos P, Javitt DC, Schroeder CE. Multisensory convergence in auditory cortex, I. Cortical connections of the caudal superior temporal plane in macaque monkeys. J Comp Neurol. 2007; 502:894–923. [PubMed: 17447261]

Van Essen DC. A tension-based theory of morphogenesis and compact wiring in the central nervous system. Nature. 1997; 385:313–318. [PubMed: 9002514]

Wallace MN, Kitzes LM, Jones EG. Chemoarchitectonic organization of the cat primary auditory cortex. Exp Brain Res. 1991; 86:527–544. [PubMed: 1761089]

Zilles K, Armstrong E, Moser KH, Schleicher A, Stephan H. Gyrification in the cerebral cortex of primates. Brain Behav Evol. 1989; 34:143–150. [PubMed: 2512000]

Zilles K, Armstrong E, Schleicher A, Kretschmann H. The human pattern of gyrification in the cerebral cortex. Anat Embryol. 1988; 79:173–179. [PubMed: 3232854]

Zilles K, Palomero-Gallagher N, Amunts K. Development of cortical folding during evolution and ontogeny. Trends Neurosci. 2013; 36:275–284. [PubMed: 23415112]

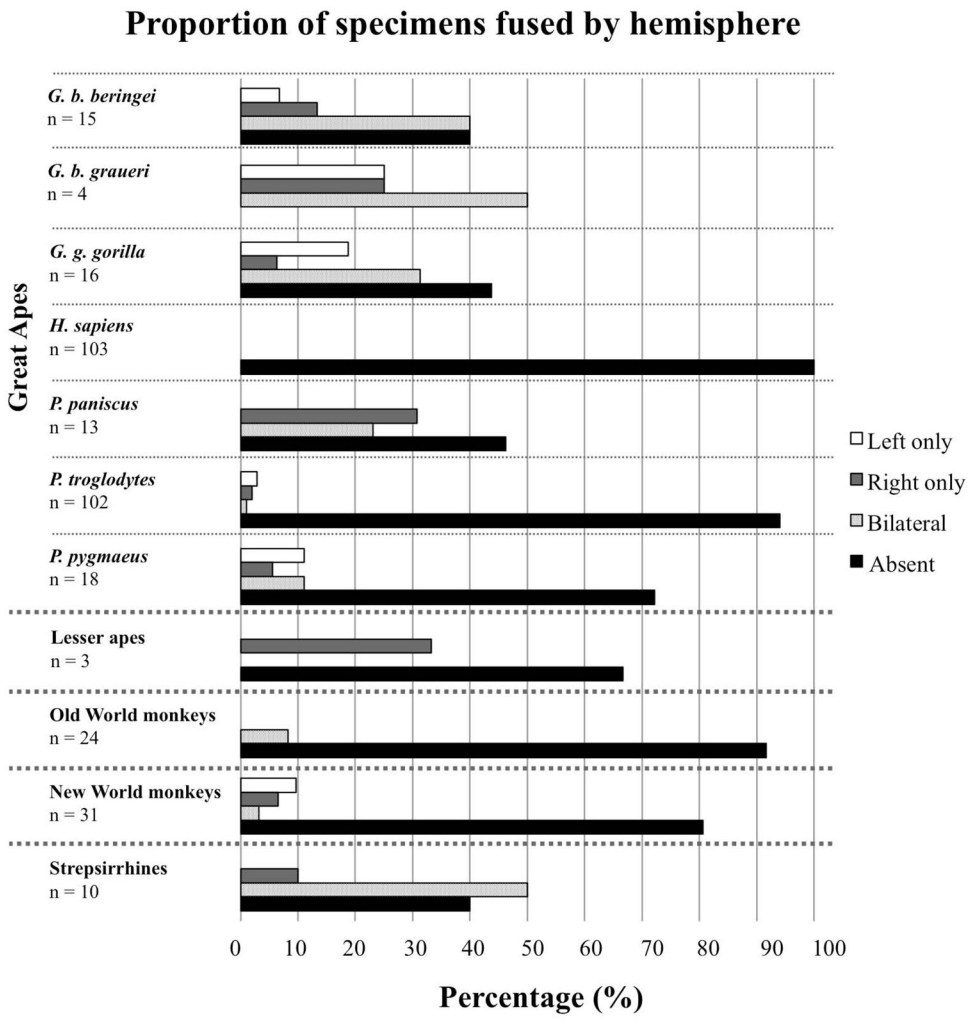

Figure 1.

Proportion of specimens that show temporo-insular fusion by hemisphere and taxon. Ape species are presented individually; other primates are presented as larger taxonomic group (Old World monkeys, New World monkeys, strepsirrhines). Specimens for which only one hemisphere was available were excluded from this analysis.

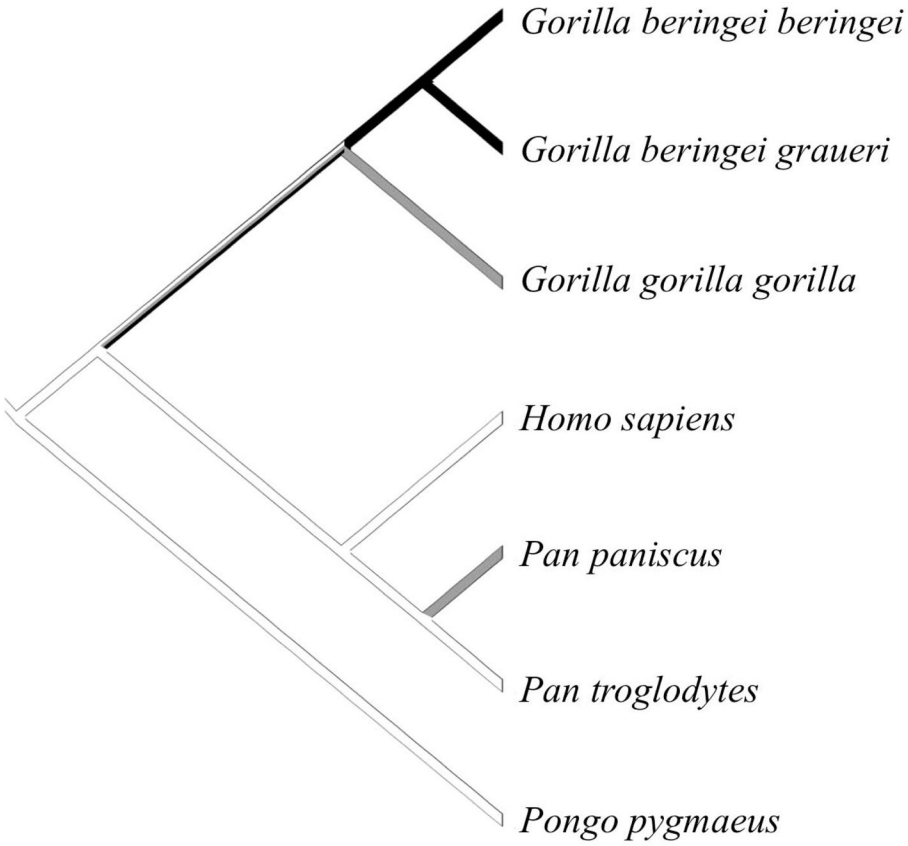

Figure 2.
Phylogenetic distribution of temporo-insular fusion in great apes. Black branches indicate fusion is common (present in 60% or more specimens). Gray branches indicate intermediate prevalence of fusion (present in 20–59% of specimens). White branches indicate fusion is rare or absent (present in fewer than 20% of specimens).

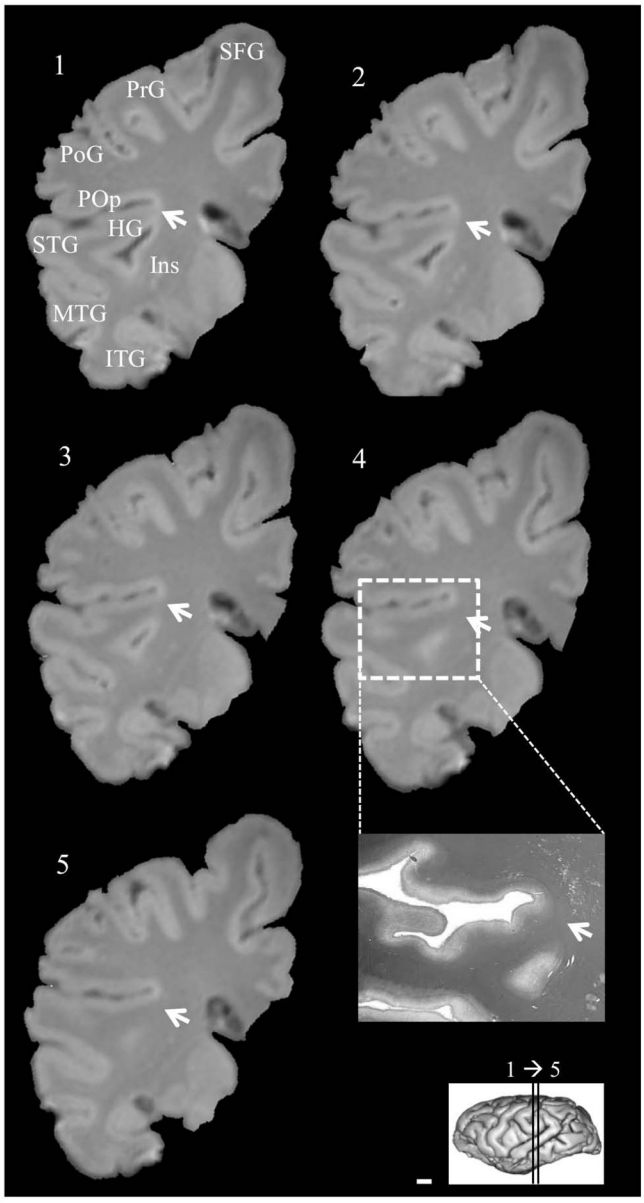

Figure 3.

Serial coronal MRI images of a fusion, including white matter, between posterior temporal lobe and posterior insula in a Grauer's gorilla (*Gorilla beringei graueri*), and tissue corresponding to coronal section 4 stained for myelin (inset). Arrows indicate point of fusion. Left hemisphere, anterior to posterior. Numbers indicate level of coronal section. Scale bar = 1 mm. HG: Heschl's gyrus. Ins: Insula. ITG: Inferior temporal gyrus. MTG: Middle temporal gyrus. PoG: Postcentral gyrus. POp: Parietal operculum. PrG: Precentral gyrus. SFG: Superior frontal gyrus. STG: Superior temporal gyrus.

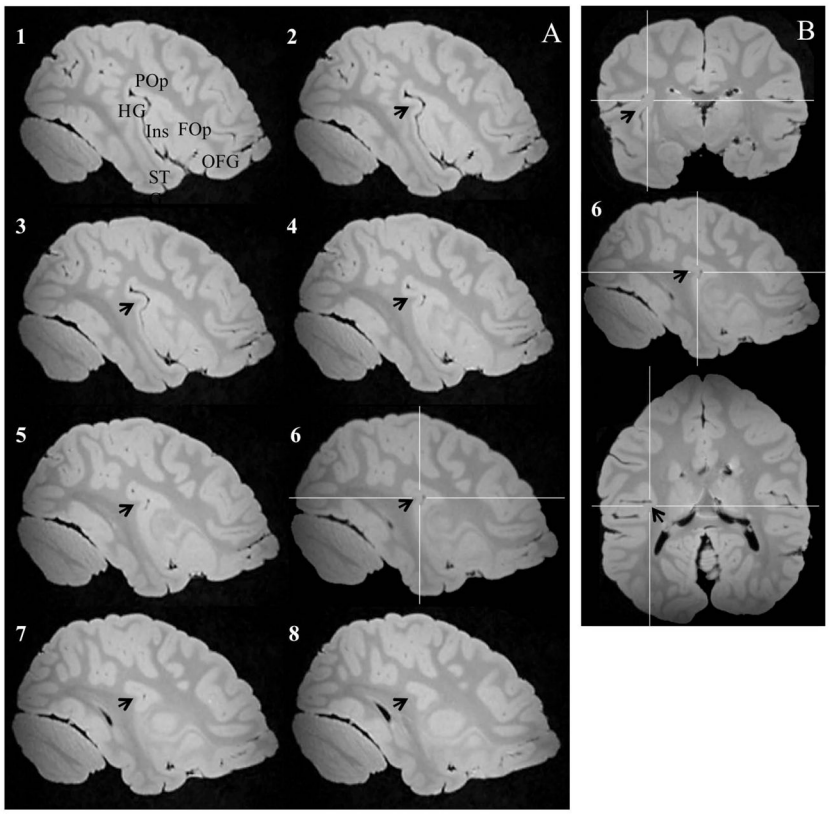

Figure 4.

A. Series of parasagittal sections in a mountain gorilla with a temporo-insular fusion. Section 1 is most lateral, section 8 most medial. Arrows indicate Heschl's gyrus. Crosshairs mark point of fusion. B. Point of fusion in the same mountain gorilla shown in cortical (top), sagittal (center), and axial (bottom) planes. Arrows indicate Heschl's gyrus. Crosshairs mark point of fusion. FOp: Frontal operculum. HG: Heschl's gyrus. Ins: Insula. ITG: Inferior temporal gyrus. OFG: Orbitofrontal gyri. POp: Parietal operculum. STG: Superior temporal gyrus.

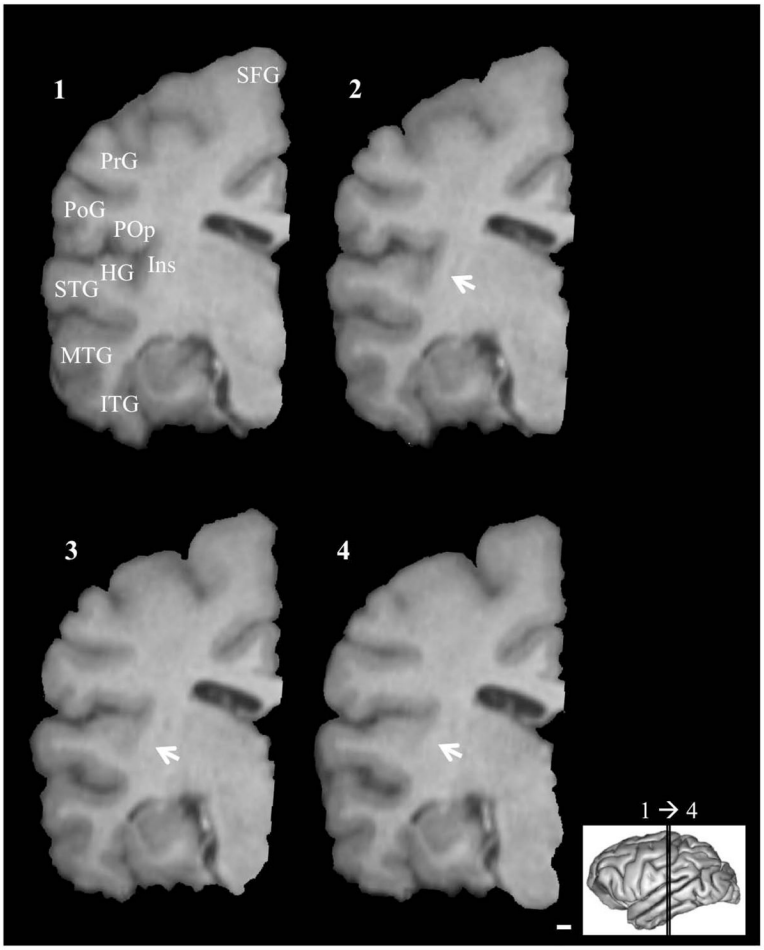

Figure 5.

Serial coronal MRI images of typical unfused posterior temporo-insular anatomy in a chimpanzee (*Pan troglodytes*). Arrows indicate site of closure of the inferior limiting sulcus without fusion. Left hemisphere, anterior to posterior. Numbers indicate level of coronal section. Scale bar = 1 mm. HG: Heschl's gyrus. Ins: Insula. ITG: Inferior temporal gyrus. MTG: Middle temporal gyrus. PoG: Postcentral gyrus. POp: Parietal operculum. PrG: Precentral gyrus. SFG: Superior frontal gyrus. STG: Superior temporal gyrus.

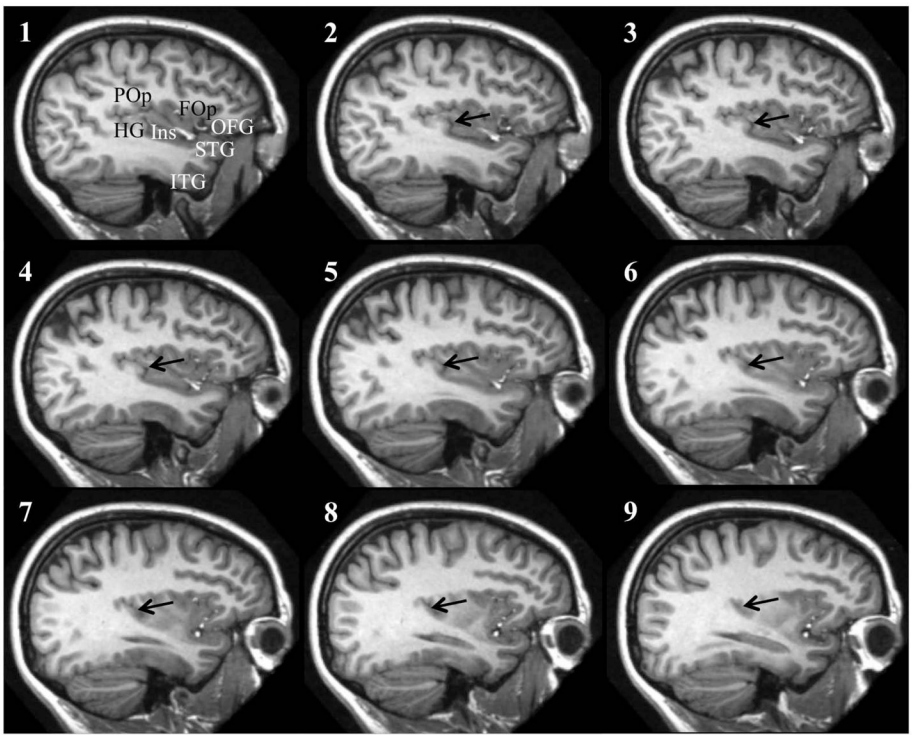

Figure 6.

Series of parasagittal sections in a human (bottom) with typical unfused temporo-insular anatomy. Section 1 is most lateral, section 9 most medial. Arrows indicate Heschl's gyrus. FOp: Frontal operculum. HG: Heschl's gyrus. Ins: Insula. ITG: Inferior temporal gyrus. OFG: Orbitofrontal gyri. POp: Parietal operculum. STG: Superior temporal gyrus.

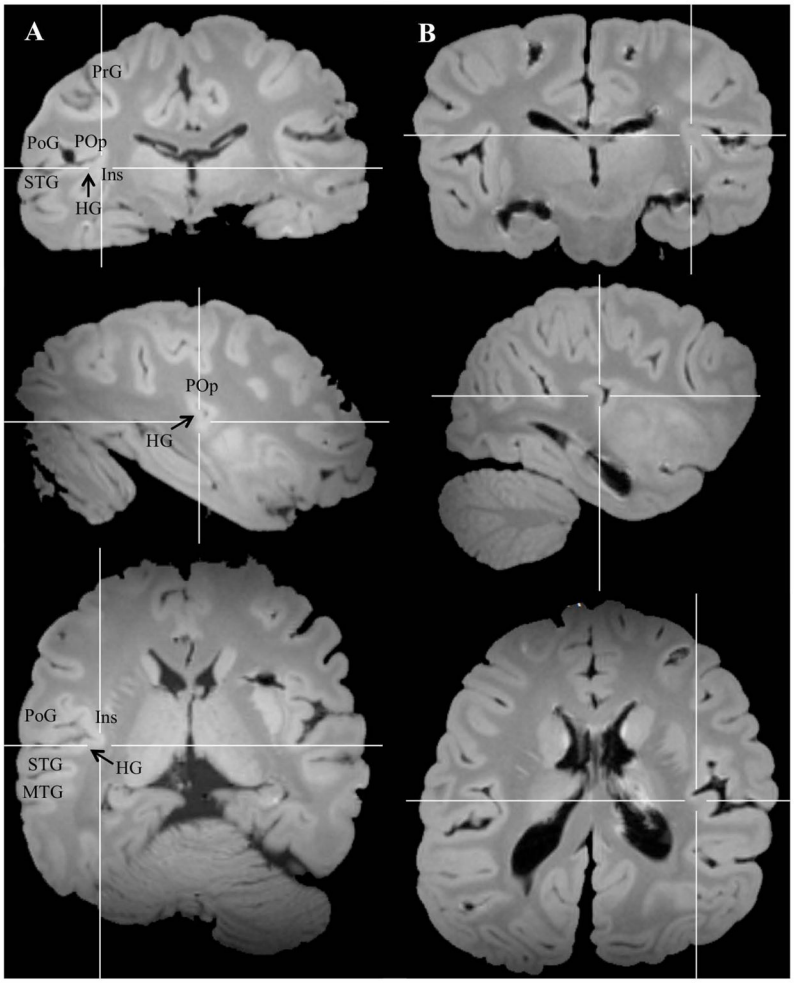

Figure 7.

Examples of fused temporo-insular anatomy in two mountain gorillas (A and B), shown in cortical (top), sagittal (center), and axial (bottom) planes. Crosshairs placed on point of fusion. HG: Heschl's gyrus. PoG: Postcentral gyrus. POp: Parietal operculum. PrG: Precentral gyrus.

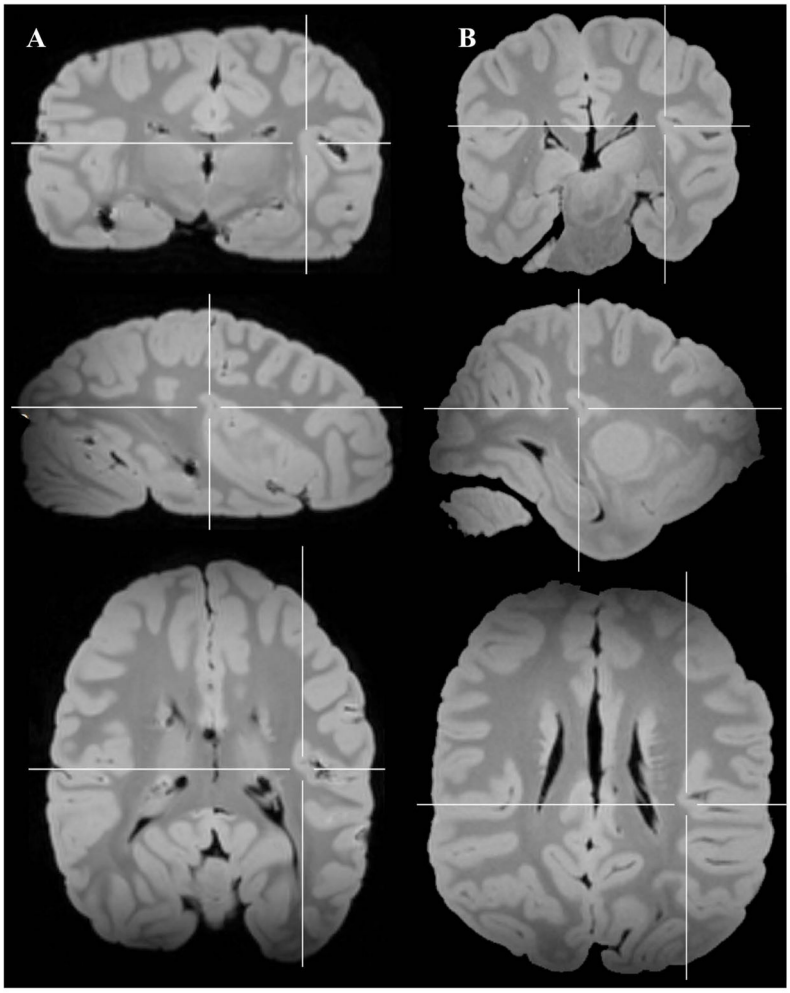

Figure 8.

Examples of fused temporo-insular anatomy in two Grauer's gorillas (A and B), shown in cortical (top), sagittal (center), and axial (bottom) planes. Crosshairs placed on point of fusion.

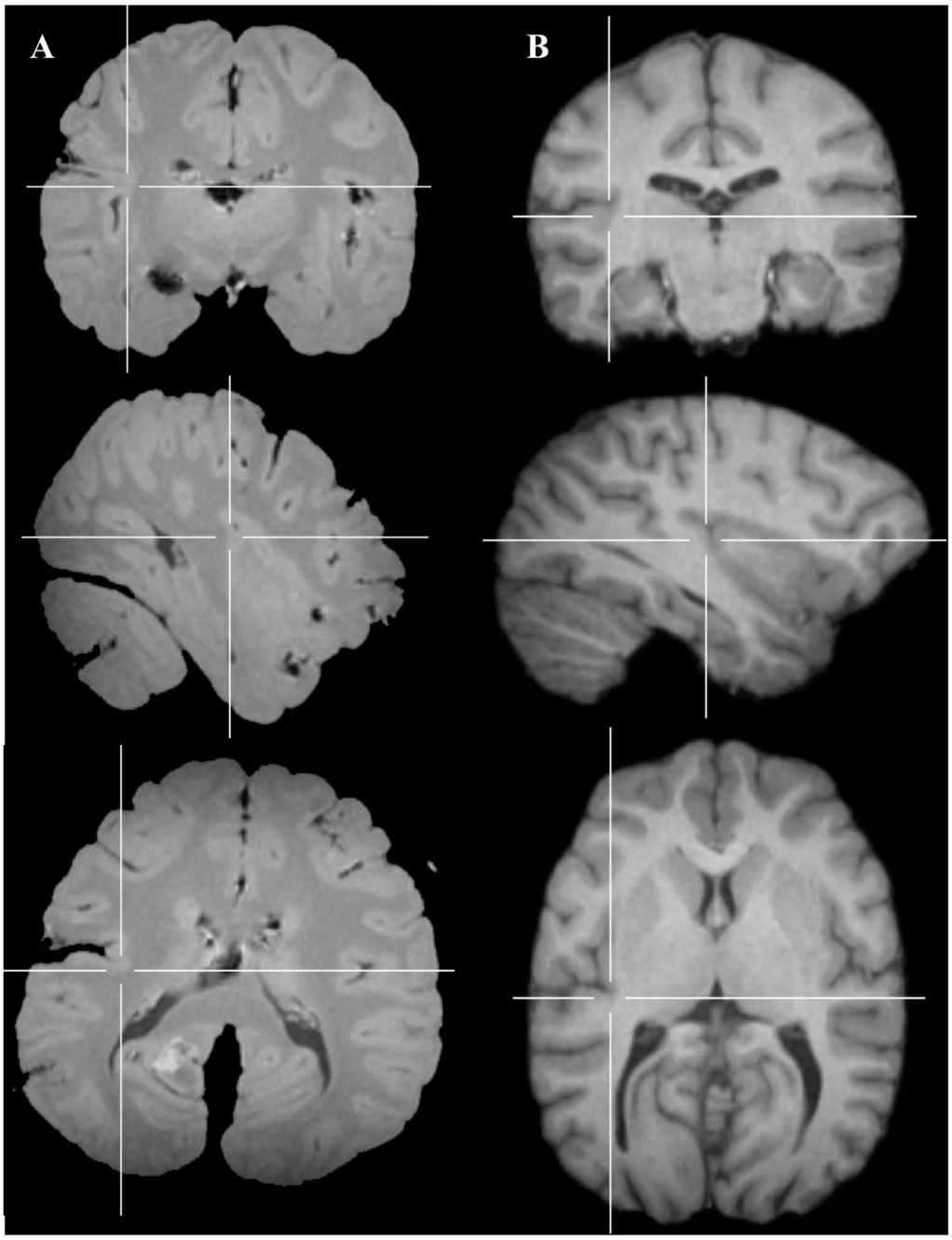

Figure 9.

Example of fused temporo-insular anatomy in a bonobo (A) and typical unfused temporo-insular anatomy in a chimpanzee (B), shown in cortical (top), sagittal (center), and axial (bottom) planes. Crosshairs placed on point of fusion in bonobo (A) and equivalent coordinates in chimpanzee (B).

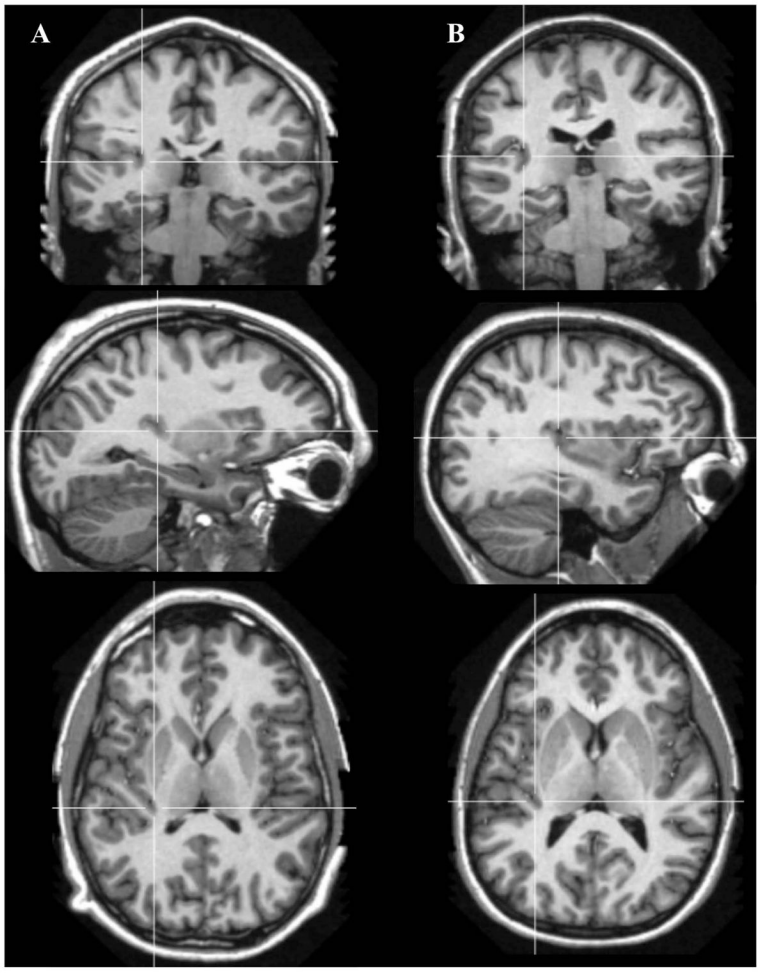

Figure 10.

Example of typical unfused temporo-insular anatomy in two humans (A and B), shown in cortical (top), sagittal (center), and axial (bottom) planes. Crosshairs placed on coordinates equivalent to those shown in Figures 5–7.

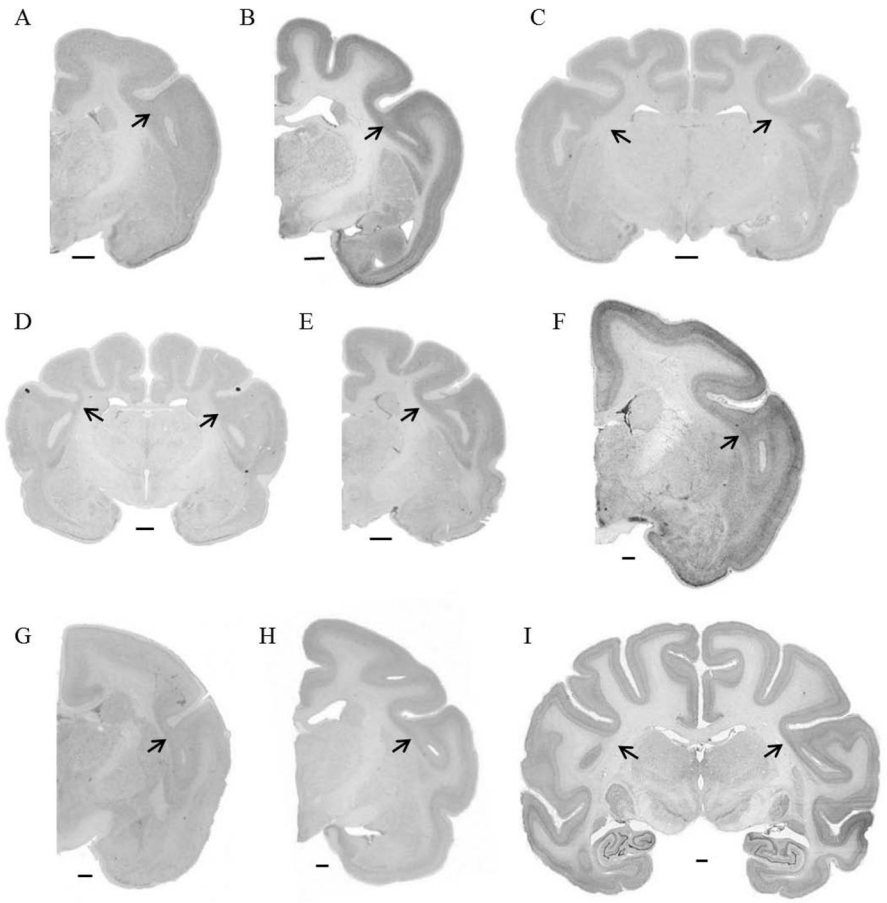

Figure 11.

Examples of fused temporo-insular anatomy across species. A. *Avahi laniger.* B. *Eulemur mongoz.* C. *Indri indri.* D. *Loris tardigradus.* E. *Varecia variegata.* F. *Aotus trivirgatus.* G. *Saguinus oedipus.* H. *Callicebus moloch.* I. *Macaca mulatta.* Scale bars = 1 mm. Arrows indicate point of fusion.

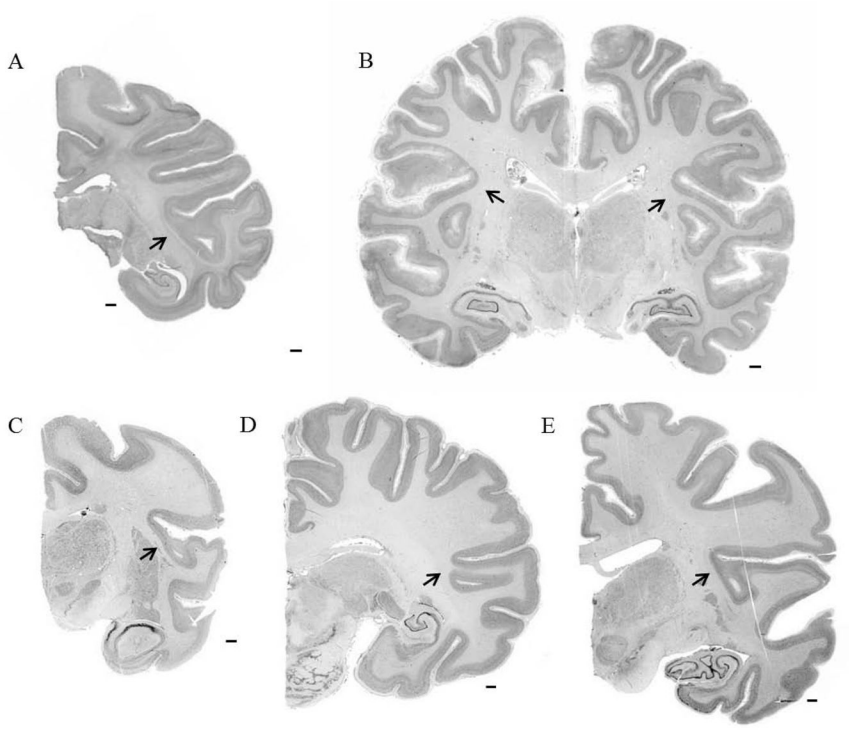

Figure 12.

Examples of fused temporo-insular anatomy across species. A. *Macaca nemestrina.* B. *Gorilla gorilla.* C. *Hylobates lar.* D. *Pan paniscus.* E. *Pan troglodytes.* Scale bars = 1 mm. Arrows indicate point of fusion.

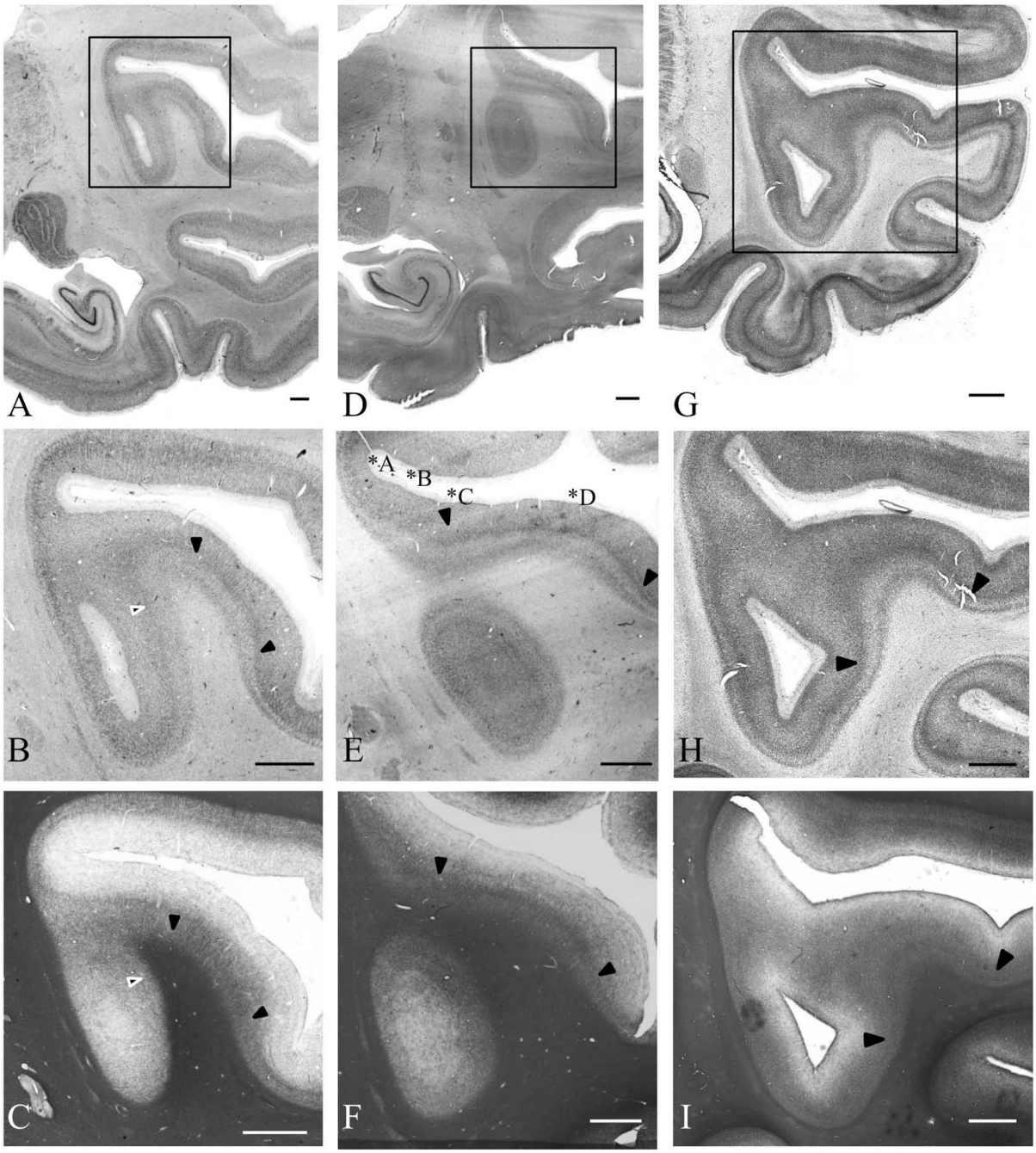

Figure 13.

Examples of temporo-insular fusion in three individuals: fusion of gray matter in a mountain gorilla (*Gorilla beringei beringei*), right hemisphere, stained for Nissl substance (A, B) and myelin (C); fusion extending into the white matter in a mountain gorilla (*Gorilla beringei beringei*), right hemisphere, stained for Nissl substance (D, E) and myelin (F); fusion of gray matter in a pigtail macaque (*Macaca nemestrina*), left hemisphere, stained for Nissl substance (G, H) and myelin (I). Scale bar = 1 mm. Solid black arrowheads demarcate likely boundaries of the core of primary auditory cortex; white outlined arrowheads (B, C)

demarcate a possible more medial boundary of primary auditory cortex in one specimen. Asterisks in panel E correspond to cortical areas shown in Figure 14.

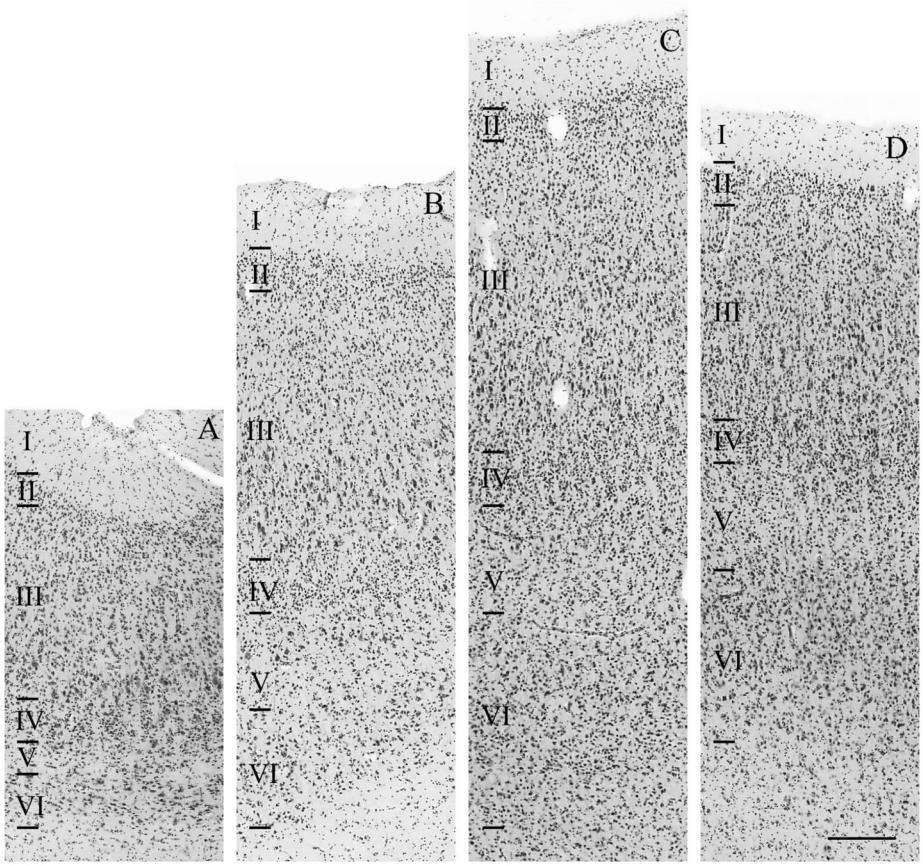

Figure 14.

Example of cytoarchitecture within a temporo-insular fusion extending into white matter in a mountain gorilla (*Gorilla beringei beringei*), right hemisphere, stained for Nissl substance. Scale bar = 250 μm. Areas shown correspond to those labeled in Fig. 13E and include dysgranular insula (A), medial belt of auditory association cortex (B), the boundary between the medial auditory belt and core of primary auditory cortex (C), and core of primary auditory cortex (D).

Table 1

Occurrence of fusion in all species, by hemisphere.

Taxon and species	Total n of individuals	Fusions in available left hemispheres	Fusions in available right hemispheres	Proportion bilateral when available
Apes				
Gorilla beringei beringei[*]	21	7/15 (47%)	12/21 (57%)	6/15 (40%)
Gorilla beringei graueri[*]	4	3/4 (75%)	3/4 (75%)	2/4 (50%)
Gorilla gorilla gorilla[*]	17	8/16 (50%)	6/17 (35%)	5/16 (31%)
Homo sapiens[*]	103	0/103	0/103	0/103
Hylobates lar	2	0/2	1/2 (50%)	0/2
Hylobates muelleri	1	0/1	NA	NA
Nomascus leucogenys[*]	1	0/1	0/1	0/1
Pan paniscus[*]	14	4/13 (31%)	7/14 (50%)	4/13 (31%)
Pan troglodytes[*]	102	3/103 (3%)	3/102 (3%)	1/102 (1%)
Pongo pygmaeus[*]	20	4/20 (20%)	3/18 (17%)	2/18 (11%)
Symphalangus syndactylus	1	0/1	NA	NA
Old World monkeys				
Cercocebus agilis	1	0/1	NA	NA
Cercopithecus mitis	1	0/1	0/1	0/1
Chlorocebus aethiops	3	0/3	0/3	0/3
Colobus angolensis	1	0/1	NA	NA
Colobus guereza	1	0/1	0/1	0/1
Macaca fascicularis	3	0/3	0/3	0/3
Macaca maura	6	0/6	NA	NA
Macaca mulatta[*]	12	2/12 (16%)	2/10 (20%)	1/10 (10%)
Macaca nemestrina	7	1/6 (17%)	0/1	0/1
Mandrillus sphinx	1	0/1	0/1	0/1
Miopithecus talapoin	1	0/1	0/1	0/1
Papio anubis	7	0/7	0/1	0/1
Procolobus badius	1	0/1	0/1	0/1
Semnopithecus entellus	1	0/1	0/1	0/1
Trachypithecus francoisi	2	0/2	NA	NA
New World monkeys				
Alouatta caraya	2	0/2	NA	NA
Alouatta palliata	1	0/1	0/1	0/1
Alouatta seniculus	1	1/1 (100%)	0/1	0/1
Aotus trivirgatus	3	0/1	1/1 (100%)	0/1
Ateles belzebuth	1	0/1	NA	NA
Callicebus moloch	1	0/1	1/1 (100%)	0/1

Taxon and species	Total n of individuals	Fusions in available left hemispheres	Fusions in available right hemispheres	Proportion bilateral when available
Callithrix jacchus	2	0/2	NA	NA
Callithrix pygmaea	2	0/2	0/2	0/2
Cebus albifrons	1	0/1	0/1	0/1
Cebus apella[*]	15	0/15	0/14	0/14
Leontopithecus rosalia	1	0/1	NA	NA
Pithecia pithecia	1	0/2	NA	NA
Saguinus geoffroyi	2	0/2	0/1	0/1
Saguinus midas	1	0/1	0/1	0/1
Saguinus oedipus	5	2/5 (40%)	0/2	0/2
Saimiri boliviensis	1	0/1	NA	NA
Saimiri sciureus[*]	6	0/6	0/5	0/5
Strepsirrhines				
Avahi laniger	1	0/1	1/1 (100%)	0/1
Cheirogaleus medius	2	0/2	NA	NA
Eulemur flavifrons	1	0/1	0/1	0/1
Eulemur mongoz	1	1/1 (100%)	0/1	0/1
Galagoides demidovii	1	1/1 (100%)	1/1 (100%)	1/1 (100%)
Indri indri	1	1/1 (100%)	1/1 (100%)	1/1 (100%)
Lemur catta	3	1/2 (50%)	1/1 (100%)	NA
Loris tardigradus	4	1/4 (25%)	1/1 (100%)	1/1 (100%)
Microcebus murinus	1	1/1 (100%)	NA	NA
Nycticebus coucang	4	0/4	0/1	0/1
Otolemur crassicaudatus	1	1/1 (100%)	1/1 (100%)	1/1 (100%)
Perodicticus potto	2	0/2	0/1	0/1
Varecia variegata	1	1/1 (100%)	1/1 (100%)	1/1 (100%)

[*] Sample includes MRI data.